

University of Nebraska - Lincoln

DigitalCommons@University of Nebraska - Lincoln

Xiao Cheng Zeng Publications

Published Research - Department of Chemistry

2010

Observation of earlier two-to-three dimensional structural transition in gold cluster anions by isoelectronic substitution:

Mau_n^- ($n=8-11$; $M=\text{Ag,Cu}$)

Lei-Ming Wang

Washington State University, Richland

Rhitankar Pal

University of Nebraska-Lincoln

Wei Huang

Brown University


Xiao Cheng Zeng

University of Nebraska-Lincoln, xzeng1@unl.edu

Lai-Sheng Wang

Brown University, Providence, Rhode Island

Follow this and additional works at: <https://digitalcommons.unl.edu/chemzeng>

 Part of the [Chemistry Commons](#)

Wang, Lei-Ming; Pal, Rhitankar; Huang, Wei; Zeng, Xiao Cheng; and Wang, Lai-Sheng, "Observation of earlier two-to-three dimensional structural transition in gold cluster anions by isoelectronic substitution: Mau_n^- ($n=8-11$; $M=\text{Ag,Cu}$)" (2010). *Xiao Cheng Zeng Publications*. 104.

<https://digitalcommons.unl.edu/chemzeng/104>

This Article is brought to you for free and open access by the Published Research - Department of Chemistry at DigitalCommons@University of Nebraska - Lincoln. It has been accepted for inclusion in Xiao Cheng Zeng Publications by an authorized administrator of DigitalCommons@University of Nebraska - Lincoln.

Observation of earlier two-to-three dimensional structural transition in gold cluster anions by isoelectronic substitution: MAu_n^- ($n=8-11$; $M=Ag, Cu$)

Lei-Ming Wang,^{1,a)} Rhitankar Pal,² Wei Huang,³ Xiao Cheng Zeng,^{2,b)} and Lai-Sheng Wang^{3,c)}

¹Department of Physics, Washington State University, Richland, Washington 99354, USA

²Department of Chemistry, University of Nebraska-Lincoln, Lincoln, Nebraska 68588, USA

³Department of Chemistry, Brown University, Providence, Rhode Island 02912, USA

(Received 9 January 2010; accepted 16 February 2010; published online 19 March 2010)

The effects of isoelectronic substitution on the electronic and structural properties of gold clusters are investigated in the critical size range of the two-dimensional (2D)-three-dimensional (3D) structural transition (MAu_n^- , $n=8-11$; $M=Ag, Cu$) using photoelectron spectroscopy and density functional calculations. Photoelectron spectra of MAu_n^- are found to be similar to those of the bare gold clusters Au_{n+1}^- , indicating that substitution of a Au atom by a Ag or Cu atom does not significantly alter the geometric and electronic structures of the clusters. The only exception occurs at $n=10$, where very different spectra are observed for MAu_{10}^- from Au_{11}^- , suggesting a major structural change in the doped clusters. Our calculations confirm that MAu_8^- possesses the same structure as Au_9^- with Ag or Cu simply replacing one Au atom in its C_{2v} planar global minimum structure. Two close-lying substitution isomers are observed, one involves the replacement of a center Au atom and another one involves an edge site. For Au_{10}^- we identify three coexisting low-lying planar isomers along with the D_{3h} global minimum. The coexistence of so many low-lying isomers for the small-sized gold cluster Au_{10}^- is quite unprecedented. Similar planar structures and isomeric forms are observed for the doped MAu_9^- clusters. Although the global minimum of Au_{11}^- is planar, our calculations suggest that only simulated spectra of 3D structures agree with the observed spectra for MAu_{10}^- . For MAu_{11}^- , only a 3D isomer is observed, in contrast to Au_{12}^- which is the critical size for the 2D-3D structural transition with both the 2D and 3D isomers coexisting. The current work shows that structural perturbations due to even isoelectronic substitution of a single Au atom shift the 2D to 3D structural transition of gold clusters to a smaller size. © 2010 American Institute of Physics. [doi:10.1063/1.3356046]

I. INTRODUCTION

There have been intense research interests on gold-containing nanostructures, motivated primarily by the discovery of unique catalytic properties of supported gold nanoparticles.¹ An atomic-level understanding of the structures and electronic properties of free gold clusters is essential to unravel the catalytic mechanisms of gold nanoparticles. During the past decade, there have been numerous experimental²⁻¹⁷ and theoretical¹⁸⁻²⁹ studies on the structural properties of small-sized neutral and charged gold clusters. One of the most intriguing findings is the planar negatively charged gold clusters (Au_n^-) for n up to 12, where the two-dimensional (2D) to three-dimensional (3D) structural transition occurs. The surprising 2D structures of Au_n^- clusters were discovered by ion mobility experiments and density functional theory (DFT) calculations,⁷ and were suggested to be a result of the strong relativistic effects of gold,^{18,22} which

reduce the Au $5d-6s$ energy gap and enhance $s-d$ hybridization. Subsequent photoelectron spectroscopy⁹ (PES) and trapped ion electron diffraction^{14,30} studies confirmed the planar structures of the small gold cluster anions and the 2D-3D structural transition at Au_{12}^- . Very recently, we further confirmed the coexistence of 2D and 3D structures in Au_{12}^- and obtained isomer-specific PES spectra using Ar tagging.³¹

On the other hand, clusters of the two lighter coinage metals, silver and copper, are known to have structures very different from gold clusters (except those smaller than the tetramer³²), and the onset of 3D structures for $Ag_n^{0/+/-}$ and $Cu_n^{0/+/-}$ appears at relatively small sizes compared to gold clusters.^{33,34} Although all the coinage atoms possess similar valence electronic characters, all with a single s -valence electron plus a completely filled d shell, their physical and chemical properties are different, such as atomic radii, ionization potentials, or electronegativities, mainly due to the much stronger relativistic effects in gold than silver and copper.¹⁸ A question arises: What would happen if one or more gold atoms in gold clusters are replaced by silver or copper? In comparison to pure gold clusters, the studies on mixed coinage-metal clusters are relatively scarce. The AgAu and CuAu dimers and some of the mixed trimers have

^{a)}Current address: Department of Physics and Astronomy and Petersen Institute for NanoScience and Engineering, University of Pittsburgh, Pittsburgh, Pennsylvania 15260.

^{b)}Electronic mail: xczen@phase2.unl.edu.

^{c)}Electronic mail: lai-sheng_wang@brown.edu

been experimentally studied using resonant two-photon ionization spectroscopy.³⁵ Joint ion mobility measurements and DFT calculations on gold-silver mixed cations (Ag_mAu_n^+ , $m+n < 6$) revealed significant charge transfers from silver to gold atoms,³⁶ in agreement with a previous DFT study.³² The stability of Au_nX_m^+ clusters ($n=1-65$, $m=1,2$; $X=\text{Cu},\text{Al},\text{Y},\text{In}$) were studied by photofragmentation and mass spectrometry, where the Cu-doped clusters for $n \leq 38$ were observed to have similar shell closures as the corresponding pure gold clusters.³⁷ Photoelectron spectra of Au–Ag binary cluster anions up to the tetramer³⁸ and of Au_nCu^- ($n=2-7$) clusters³⁹ have been reported at a photon energy of 4.661 eV. Recently our combined PES and DFT studies have shown that CuAu_{16}^- and AgAu_{16}^- are endohedral cage clusters,^{40,41} similar to the golden cage Au_{16}^- rather than Au_{17}^- . However, we found that the smaller clusters $M\text{Au}_n^-$ ($M=\text{Ag},\text{Cu}$, $n=6,7$) have similar spectra and structures as the pure Au_7^- and Au_8^- clusters, respectively, with the same total number of atoms.⁴² Theoretically, the dimers and trimers of mixed coinage metals have been calculated using the 19-electron effective core potential,⁴³ as well as at the level of coupled-cluster with single and double and perturbative triple excitations [CCSD(T)].⁴⁴ Structures of single Cu atom doped gold clusters Au_nCu^- in the size range of $n=14-20$ have been calculated.⁴⁵ DFT investigations of geometric and electronic structures of small Au–Ag binary clusters with varying component Au_mAg_n (usually $m+n \leq 10$) have been reported by several groups.^{32,46,47} Larger Ag–Au and Cu–Au bimetallic systems have also been studied computationally.⁴⁸⁻⁵⁰

In the current study, we report a combined PES and DFT investigation on a series of small gold cluster anions doped with a single Ag or Cu atom in the critical size range where the 2D-3D structural transition occurs, namely, AgAu_n^- and CuAu_n^- ($n=8-11$). We chose this size range to specifically probe how the isoelectronic substitutions would affect the stability of the planar gold clusters and the 2D-3D transition. We found that the 2D-3D transition occurs at a smaller size in both cases by one atom in $M\text{Au}_{10}^-$.

II. EXPERIMENTAL METHODS

The experiment was performed on a magnetic-bottle PES apparatus equipped with a laser vaporization supersonic cluster beam source, details of which have been published elsewhere.⁵¹ The AgAu_n^- and CuAu_n^- clusters were produced by laser vaporization of an Au/Ag or Au/Cu mixed disk target containing about 7% Ag or Cu, respectively. Negatively charged clusters were extracted from the cluster beam perpendicularly and were analyzed using a time-of-flight mass spectrometer. Clusters of interest were mass-selected and decelerated before being intercepted by a 193 nm laser beam from an ArF excimer laser for photodetachment. The content of the dopant (Ag or Cu) in the target was carefully tuned to low concentrations such that multiple dopings were minimized and the $M\text{Au}_n^-$ series with a single dopant atom was optimized in order to achieve clean selections. Photoelectrons were collected and measured using a magnetic-bottle time-of-flight electron energy analyzer, and calibrated

by the known spectra of Au^- . The resolution of the apparatus was $\Delta E/E \sim 2.5\%$, i.e., about 25 meV for 1 eV electrons.

III. THEORETICAL METHODS

The search for the global-minimum structures of $M\text{Au}_n^-$ ($n=8-11$; $M=\text{Ag},\text{Cu}$) and Au_{10}^- were performed using the basin-hopping (BH) global optimization technique coupled with DFT calculations.^{52,53} Generalized gradient approximation in the Perdew–Burke–Ernzerhof (PBE) functional form was chosen.⁵⁴ Two BH programs, developed independently by the UNL group⁵⁵ and Huang *et al.*,⁴² were employed and both gave consistent sets of low-lying isomers. Several BH searches were carried out using various randomly selected initial structures. Because of the limited accuracies in energetics in the DFT calculations, we simulated the photoelectron spectra for all low-lying isomers within 0.2 eV of the most stable isomer in order to compare with the experimental data.

We recently found that the inclusion of spin-orbit (SO) effects⁵⁶ is essential to achieve quantitative agreement between simulated and measured photoelectron spectra for Au clusters.^{42,57} In the current work, we used the PBE0 hybrid functional and CRENB� basis set (i.e. the large effective-core-potential orbital basis for use with the small core potentials) including SO effects, as implemented in NWChem 5.1.1,^{58,59} to calculate the photoelectron spectra of the low-lying isomers. First, the relative energies and rankings of all the selected low-lying isomers of each $M\text{Au}_n^-$ and Au_{n+1}^- from the BH searches were reoptimized using the PBE0/CRENB� level of theory. Next, the first vertical detachment energies (VDEs) of the anion clusters were calculated at the PBE0/CRENB�(SO) level, as the energy difference between the optimized anion isomer and the neutral at the corresponding anion geometry. The binding energies of deeper orbitals were then added to the first VDE to approximate the higher binding energy detachment features. Each peak was then fitted with a Gaussian of width 0.04 eV to yield the simulated spectrum to be compared to the experimental photoelectron spectrum.

IV. EXPERIMENTAL RESULTS

The photoelectron spectra of $M\text{Au}_n^-$ from $n=8$ to 11 and $M=\text{Ag}$ and Cu are presented in Figs. 1–4, respectively, along with those of the corresponding pure Au_{n+1}^- gold clusters⁹ for comparison. The low-lying isomers that yielded simulated spectra in best agreement with the experiment are also shown, as will be discussed in Sec. V. The first VDEs for the major isomers of the doped clusters are given in Table I and are compared to those of pure gold clusters and the calculated VDE values.

- (1) $M\text{Au}_8^-$. The PES spectrum of Au_9^- [Fig. 1(a)] displays two intense and sharp peaks (X and A) around 4 eV, followed by a large energy gap and more congested higher binding energy bands.⁹ The spectra of AgAu_8^- and CuAu_8^- resemble that of Au_9^- , both featuring two sharp and intense bands at lower binding energies and the characteristic energy gap. This observation suggests

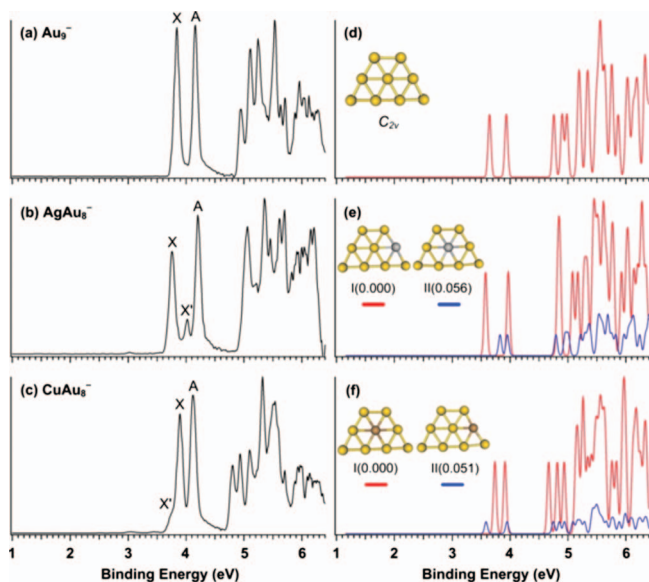


FIG. 1. Experimental [left, (a)–(c)] and simulated [right, (d)–(f)] photoelectron spectra (based on PBE0/CRENBL level) of Au_9^- , AgAu_8^- , and CuAu_8^- . The insets show the corresponding structures.

that in MAu_8^- the Ag or Cu atom simply substitutes one Au atom in Au_9^- without significantly altering the atomic and electronic structure of the parent gold cluster. However, an additional weak feature (labeled X') is clearly observed in the spectra of both AgAu_8^- [Fig. 1(b)] and CuAu_8^- [Fig. 1(c)], indicating the presence of *multiple* isomers with different structures in the doped clusters. This is not surprising, considering the fact that there may be energetically close multiple substitution sites available in the structure of Au_9^- , which can give rise to similar structures with slightly different electronic properties.

- (2) MAu_9^- . Au_{10}^- has been the focus of a recent study,⁶⁰ revealing contributions from at least four structural iso-

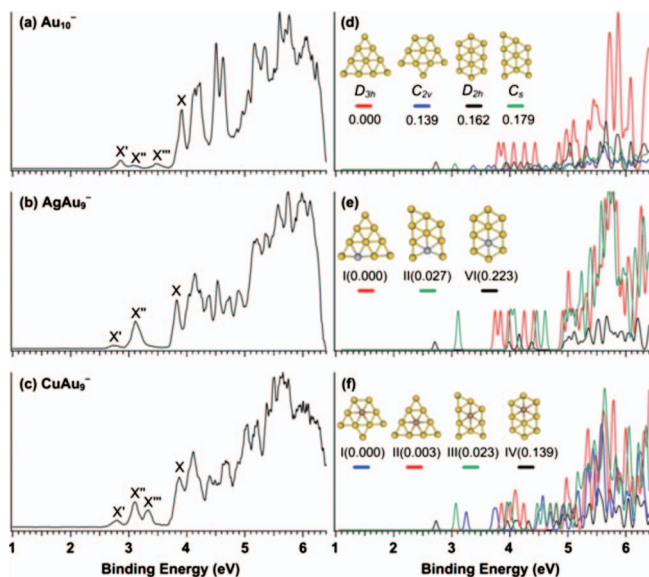


FIG. 2. Experimental [left, (a)–(c)] and simulated [right, (d)–(f)] photoelectron spectra of Au_{10}^- , AgAu_9^- , and CuAu_9^- . The insets show the corresponding structures.

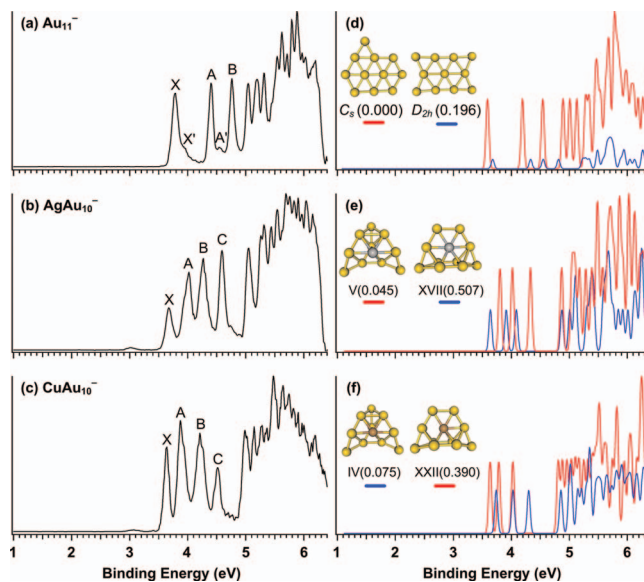


FIG. 3. Experimental [left, (a)–(c)] and simulated [right, (d)–(f)] photoelectron spectra of Au_{11}^- , AgAu_{10}^- and CuAu_{10}^- . The insets show the corresponding structures.

mers by Ar tagging and O_2 titration. The major features of the spectrum [X and the higher binding energy part in Fig. 2(a)] show very high binding energies and are known to come from the equal lateral triangular D_{3h} ground state of Au_{10}^- , whose corresponding neutral species Au_{10} possesses a triplet ground state and thus lacks an HOMO-LUMO gap (i.e., the gap between the highest occupied molecular orbital and lowest unoccupied molecular orbital). The major isomer of Au_{10}^- was shown to be unreactive toward O_2 .⁶⁰ The weak features at the low binding energy part (X' , X'' , and X''') were shown to come from three different structural isomers. The carriers of X' and X'' have been identified tentatively,⁶⁰ whereas that for X''' is still unknown.

At first glance, the spectra of AgAu_9^- and CuAu_9^- seem to be different from that of Au_{10}^- , because the first peak with appreciable intensity (X'') in the doped systems appears at much lower binding energies and gives the appearance of a HOMO-LUMO gap relative to the X band in AgAu_9^- and CuAu_9^- . In addition, the spectra of AgAu_9^- and CuAu_9^- show much more congested spectral features beyond 4 eV in comparison to that of Au_{10}^- . However, a careful examination suggests that the low binding energy peaks in the spectra of AgAu_9^- (X' and X'') and CuAu_9^- (X' , X'' , and X''') may derive from isomers similar to those populated for Au_{10}^- , except that their relative intensities may have enhanced in the doped systems. Indeed, the X band in all three spectra (Fig. 2) appears to be identical with similar peak positions and shape. This observation suggests that the dominant isomer in the doped systems is derived from the global minimum D_{3h} Au_{10}^- . The relative population of the doped clusters derived from the low-lying isomers of Au_{10}^- may be enhanced, giving rise to the more complicated spectral patterns observed for AgAu_9^- and CuAu_9^- in the high binding energy range.

- (3) MAu_{10}^- . The spectrum of Au_{11}^- [Fig. 3(a)] displays six characteristic detachment bands in the binding energy range between 3.5 and 5.5 eV, with the three low binding energy bands (*X*, *A*, and *B*) being well separated and the three higher binding energy bands between 5.0 and 5.5 eV being more closely spaced. Two weak features (*X'* and *A'*) that were not identified in our previous PES study⁹ are also discernible as tails on bands *X* and *A*, respectively, suggesting population of minor isomers. The spectra of $AgAu_{10}^-$ [Fig. 3(b)] and $CuAu_{10}^-$ [Fig. 3(c)] are similar to each other, both displaying four well resolved peaks between 3.5 and 4.5 eV followed by an energy gap and more congested signals at higher binding energies. We note that bands *A* and *B* in the spectra of $AgAu_{10}^-$ and $CuAu_{10}^-$ are apparently broader and seem to contain fine structures, which are due to either overlaps of multiple detachment transitions or contributions from different isomers. The spectral patterns of the doped clusters MAu_{10}^- are completely different from that of Au_{11}^- , suggesting that the Ag/Cu substitution may have significantly altered the planar structures of the parent gold cluster. The similar spectral patterns of $AgAu_{10}^-$ and $CuAu_{10}^-$ suggest that the two doped clusters should have similar structures, though they are most likely different from that of Au_{11}^- .
- (4) MAu_{11}^- . Au_{12}^- is the critical cluster size for the 2D-3D structural transition of anion gold clusters, where isomers of both dimensionalities have been shown to be present in the cluster beam.^{7,9,31} Using Ar tagging, we have recently obtained isomer-specific PES spectra for Au_{12}^- .³¹ The main isomer, that gives rise to band *X* in the spectrum of Au_{12}^- [Fig. 4(a)], corresponds to the 3D structure, whereas the weak band *X'* comes from the 2D isomer, which should be slightly higher in energy than the global minimum 3D structure.^{30,31} The spectra of $AgAu_{11}^-$ [Fig. 4(b)] and $CuAu_{11}^-$ [Fig. 4(c)] are nearly identical to that of the 3D isomer of Au_{12}^- in terms of

both spectral patterns and electron binding energies. Interestingly, the weak features associated with the 2D isomer in Au_{12}^- do not exist in the spectra of MAu_{11}^- . These observations indicate unequivocally that the 3D structures for MAu_{11}^- derived from the 3D isomer of Au_{12}^- become much more stable than those derived from the planar isomer of Au_{12}^- . Thus, the spectra of $AgAu_{11}^-$ and $CuAu_{11}^-$ are isomerically pure without contributions from the 2D isomers. The similarity between the spectra of MAu_{11}^- and that of the 3D isomer of Au_{12}^- suggests that the substitution by one Ag/Cu atom does not change appreciably the 3D structure of the parent gold cluster.

V. THEORETICAL RESULTS AND DISCUSSIONS

In this section, we present the theoretical results of MAu_n^- and compare the simulated PES spectra with the experimental data in order to understand how the isoelectronic substitution by a Ag or Cu atom affects the structures of the Au_{n+1}^- clusters. Since simulated PES spectra with the inclusion of SO effects have not been reported for gold clusters in the size range of Au_9^- – Au_{12}^- , they are presented here as references. We have found that the inclusion of SO effects can yield simulated PES spectra in much better agreement with the experimental PES data,^{42,57} making it possible to identify structures with much higher confidence on the basis of the simulated PES spectra. This is important because of the limited accuracy in the DFT-based energetic information among closely lying structural isomers.

- (1) Au_9^- and MAu_8^- . Au_9^- has been previously shown to possess a C_{2v} planar structure,^{7,9} as depicted in the inset of Fig. 1(d). Our current calculations confirm this structure as the global minimum and its simulated PES spec-

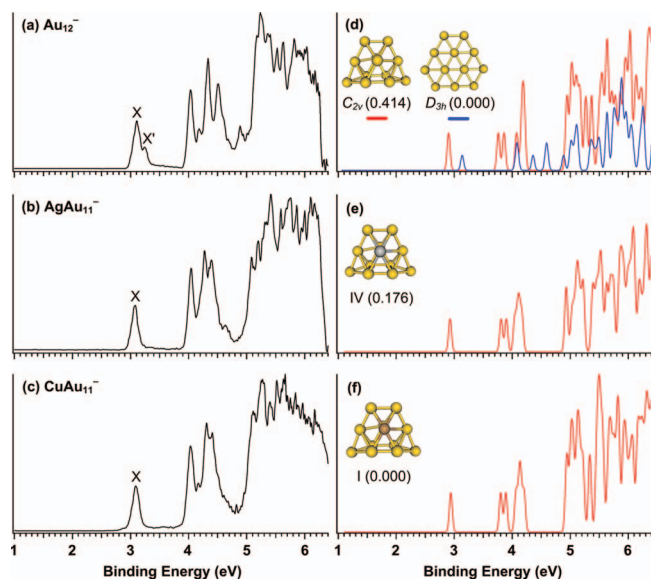


FIG. 4. Experimental [left, (a)–(c)] and simulated [right, (d)–(f)] photoelectron spectra of Au_{12}^- , $AgAu_{11}^-$, and $CuAu_{11}^-$. The insets show the corresponding structures.

TABLE I. Experimental and calculated (PBE0/CRENBL) vertical detachment energies (VDE) of MAu_n^- and Au_{n+1}^- clusters (for the major isomer if there are multiple isomers) ($M=Ag, Cu$, $n=8-11$). (Experimental data for the pure gold clusters are from Ref. 9.)

n	Species	VDE (eV)	
		Exp. ^a	Cal.
8	Au_9^-	3.83(2)	3.64
	$AgAu_8^-$	3.75(5)	3.58
	$CuAu_8^-$	3.89(5)	3.74
9	Au_{10}^-	3.91(2)	3.80
	$AgAu_9^-$	3.82(3)	3.72
	$CuAu_9^-$	3.86(5)	3.85
10	Au_{11}^-	3.80(2)	3.59
	$AgAu_{10}^-$	3.67(3)	3.64
	$CuAu_{10}^-$	3.64(5)	3.63
11	Au_{12}^-	3.06(2)	2.89
	$AgAu_{11}^-$	3.08(4)	2.93
	$CuAu_{11}^-$	3.09(5)	2.94

^aNumbers in parentheses represent the uncertainty in the last digits.

trum [Fig. 1(d)] agrees well with the experiment: The characteristic doublet peaks in the low binding energy range and the following energy gap are well reproduced. The computed first VDE, however, underestimates the VDE by about 0.2 eV (Table I).

The experimental spectra suggest that MAu_8^- should have similar structures as Au_9^- . Apparently, there are five different sites for substitution in the C_{2v} structure of Au_9^- , which may result in close-lying isomers for the doped clusters. Indeed, our BH searches revealed that the lowest-energy structure for $AgAu_8^-$ is similar to that of Au_9^- , in which an Au atom on an edge site is replaced by an Ag atom [structure I, Fig. 1(e)]. Its simulated spectrum [Fig. 1(e)] agrees very well with the main experimental PES features. A center-substituted structure [II, Fig. 1(e)] was found to be the second lowest-lying isomer, only 0.056 eV above the global minimum, and its simulated spectrum reproduces the weak feature X' in the experiment.

For $CuAu_8^-$, the center-substituted structure with C_{2v} symmetry [I, Fig. 1(f)] was found to be the lowest-energy isomer, while the edge-substituted isomer (II) becomes a low-lying isomer, which is 0.051 eV higher in energy. The simulated spectra for these two isomers [Fig. 1(f)] are again in excellent agreement with the experimental data. The center and edge site substitutions produce two nearly degenerate isomers, which are competing for the global minimum and are both populated in the MAu_8^- beams, but the relative stabilities of the two isomers are reversed between the Ag and Cu substitutions. It seems that the Cu atom with a smaller size prefers the *center* site slightly while the Ag atom favors the *edge* site. We note that substitution on the edge site has resulted in some slight local structural distortions. Specifically, the Ag atom in $AgAu_8^-$ is slightly popped outward [structure I, Fig. 1(e)], while in $CuAu_8^-$ the Cu atom is apparently shrunk inward [structure II, Fig. 1(f)] as a result of the different atomic sizes of Cu and Ag. The simulated PES spectra are somewhat sensitive to the different substitution sites: the edge substitution seems to enhance the spacing between the first two PES bands, whereas the center substitution decreases the spacing between the first two PES bands in the simulated spectra. This structural sensitivity in the simulated spectra is in perfect agreement with the experimental observations, lending significant credence to the identified structures.

- (2) Au_{10}^- and MAu_9^- . Au_{10}^- is an interesting cluster with numerous planar low-lying isomers, which possess different chemical reactivities toward O_2 ; at least *four* isomers have been identified recently to coexist in the cluster beam using Ar tagging and O_2 titration by Huang and Wang.⁶⁰ The dominant isomer and the global minimum of Au_{10}^- is a D_{3h} planar triangular structure [inset in Fig. 2(d)]. The neutral D_{3h} Au_{10} possesses an open-shell triplet electronic state with a very high electron affinity (EA) and accounts for the major spectral features observed in the PES spectrum [Fig. 2(a)].⁶⁰ The high EA of the D_{3h} isomer is due to the open shell

nature of its neutral—the high symmetry of this isomer results in a degenerate highest occupied molecular orbital (HOMO) which is half-filled. The high binding energy of Au_{10}^- has also been explained using a 2D shell model.^{61,62} Two of the weak low binding energy peaks (X' and X'') were tentatively assigned to two low-lying isomers according to previous calculations,⁹ while the X''' band was suggested to come from a yet unidentified fourth isomer in the recent study.⁶⁰ In the current study, we did extensive BH structural searches for Au_{10}^- . Three low-lying isomers were found within 0.2 eV above the D_{3h} ground state, as displayed in the inset of Fig. 2(d). Our calculations confirm that the global minimum of Au_{10}^- is the D_{3h} triangular structure, whose simulated spectrum reproduces well the major spectral features in the experiment [Fig. 2(d)].

The D_{2h} isomer [Fig. 2(d)], 0.162 eV above the global minimum from the current calculations, was identified to be a low-lying isomer previously^{7,9} and assigned to be responsible for the X' band by Huang and Wang.⁶⁰ Our calculations show that the D_{2h} isomer possesses a large HOMO-lowest unoccupied molecular orbital (LUMO) gap and gives rise to a very low first VDE in good agreement with the experimental data, confirming the previous assignment. The second band X'' was tentatively assigned to a C_{2h} isomer by Huang and Wang,⁶⁰ on the basis of a previous calculation.⁹ However, in the current study we found a new C_s structure [Fig. 2(d)], which should be responsible for the X'' band. This isomer is 0.18 eV above the global minimum, but 0.17 eV lower in energy than the previously suggested C_{2h} isomer, and yields a first VDE in good agreement with the X'' band. As will be shown below, this structure turns out to be quite important in the doped clusters. Finally, we found another new C_{2v} low-lying isomer [Fig. 2(d)], which is only 0.139 eV higher in energy than the global minimum according to the current calculations. This isomer yields a first VDE in good agreement with the X''' band. The simulated spectra of all *four* Au_{10}^- isomers are shown in Fig. 2(d), and together they agree well with the measured spectrum. The coexistence of so many low-lying isomers for the small-sized gold cluster Au_{10}^- is quite unprecedented. Interestingly, all the low-lying isomers of Au_{10}^- can be viewed as a central D_{6h} Au_7^- unit with the additional three Au atoms arranged in different positions around it, even though Au_7^- itself does not possess a D_{6h} global minimum.^{7,9,42} Our theoretical results show that the doped clusters MAu_9^- have similar planar structures as Au_{10}^- . For $AgAu_9^-$, the two lowest-lying isomers [structures I and II, Fig. 2(e)] can be viewed as derived from the D_{3h} and C_s structures of Au_{10}^- , respectively, by substitution of an Au atom with an Ag atom, both at the edge sites. These two isomers are nearly degenerate in energy (structure II is only 0.027 eV higher), thus both are expected to have substantial population in the cluster beam. Indeed, the simulated spectra for these two isomers [Fig. 2(e)] reproduce well all the major experimental PES features. The structure II gives rise to band X'' , which is quite

intense. The weak low binding energy feature X' should correspond to another isomer. Although a number of planar structures are obtained from the BH searches, only the isomer derived from the D_{2h} structure of Au_{10}^- yields a very low VDE, which is in good agreement with the weak feature X' . This isomer corresponds to structure VI in our calculations, which is 0.223 eV above the global minimum. The relatively high energy of structure VI is consistent with its weak intensity in the experimental spectrum.

For the Cu substitution, the four low-lying isomers [inset in Fig. 2(f)] are identical to those of the Au_{10}^- parent: in each case Cu substitutes the central Au atom. The first three isomer structures (I, II, and III) of CuAu_{10}^- , corresponding to the C_{2v} , D_{3h} , and C_s isomers of Au_{10}^- , respectively, are very close in energy, and a superposition of their simulated spectra reproduces well the major PES features observed experimentally. Again, the D_{2h} - Au_{10}^- derived isomer, which is 0.139 eV above the global minimum, yields the lowest VDE, in good agreement with the weak X' feature [Fig. 2(c)].

- (3) Au_{11}^- and MAu_{10}^- . The global minimum of Au_{11}^- is shown to possess a C_s structure [Fig. 3(d)],^{7,9} which can be viewed as built from the D_{2h} isomer of Au_{10}^- by adding one more Au atom at an edge site. The current work confirms this result and the simulated spectrum of the C_s global minimum with the inclusion of SO effect is in excellent agreement with the experimental spectrum of Au_{11}^- . A previously reported⁹ low-lying isomer with D_{2h} symmetry [Fig. 3(d)] was calculated to be 0.196 eV above the global minimum in the current study. The simulated spectrum of the D_{2h} structure agrees well with the weak features X' and A' observed experimentally [Fig. 3(a)].

For MAu_{10}^- , we carried out extensive BH searches by starting from several randomly built initial structures. In addition, we considered every possible substitution site in the global-minimum structure of Au_{11}^- . The obtained lowest-lying 20 and 28 structures, respectively, for AgAu_{10}^- and CuAu_{10}^- , are sorted out in supplemental materials Figs. S1 and S2, along with their simulated spectra.⁶³ For AgAu_{10}^- , the first few low-lying isomers are dominant by 2D structures, which can be viewed as derived from the C_s structure of Au_{11}^- . Only one 3D isomer (structure V, Fig. S1) is found to be competitive in energy (0.045 eV above the lowest-lying isomer). For CuAu_{10}^- , the two lowest-lying structures are both 3D. A center-substituted 2D structure (III) and another 3D structure (IV) are found to be very close in energy to the global minimum (Fig. S2). However, as can be seen from Figs. S1 and S2, none of the simulated spectra for a single isomer agrees with the experimental PES spectra for either AgAu_{10}^- or CuAu_{10}^- , consistent with the experimental observations that the spectra of AgAu_{10}^- and CuAu_{10}^- likely contain contributions from multiple isomers. As discussed above in the experimental results, the broad nature of bands A and B [Figs. 3(b) and 3(c)] suggests that they could be due to overlap of multiple transitions.

Among the extensive set of low-lying structures for AgAu_{10}^- , the best agreement with experiment was obtained by the superposition of two 3D isomers, structures V and XVII [Fig. 3(e)]. The structure V is only 0.045 eV higher in energy and can be viewed as degenerate with structure I, while structure XVII is a higher-lying isomer (0.507 eV above structure I) [Fig. S1]. Two similar 3D structures for CuAu_{10}^- also yield a superposition of simulated spectra in best agreement with the experiment [Fig. 3(f)]. Again, while structure IV of CuAu_{10}^- is only 0.075 eV higher in energy and is competing for the global minimum, structure XXII has a relatively higher energy of 0.390 eV above structure I (Fig. S2). It is known that DFT/PBE energies calculated for gold clusters around the 2D-3D transition point show large uncertainties.^{30,64,65} That is possibly one reason that structure XVII of AgAu_{10}^- and structure XXII of CuAu_{10}^- are observed in the experiment, though their relative energies are calculated to be high according to the DFT/PBE0 calculations, i.e., the DFT/PBE0 calculations underestimate the stability of the 3D structures.

Two recent theoretical works suggest that DFT calculations with M06 or M06-L functionals can correctly predict the relative energies for gold clusters.^{64,65} We recalculated single-point energies of the two assigned 3D structures, as well as a few low-lying isomers of MAu_{10}^- at the M06-L/CRENBL(SO) level of theory, using the NWChem 5.1.1 software package. The two identified structures for both AgAu_{10}^- (structures V and XVII) and CuAu_{10}^- (structures IV and XXII) indeed turn out to be the two lowest-energy isomers (among those checked) at this level (see Figs. S1 and S2). Therefore, both experimental and theoretical data strongly suggest that, in contrast to the planar Au_{11}^- , the global minima of MAu_{10}^- are 3D. Thus, the isoelectronic substitution by Ag or Cu shifts the 2D-3D structural transition to the 11-atom clusters, AgAu_{10}^- and CuAu_{10}^- , compared with Au_{12}^- in the bare gold clusters. Note in passing that the PBE0/CRENBL(SO) level of theory typically underestimates the VDE of 2D clusters by 0.1–0.2 eV, but only slightly underestimates VDE of 3D clusters AgAu_{10}^- and CuAu_{10}^- (see Table I). This explains why the computed VDE of substituted clusters (which are 3D) can be even larger than that of Au_{11}^- cluster (which is 2D).

- (4) Au_{12}^- and MAu_{11}^- . It is now well established that Au_{12}^- is the critical size, where the 2D-3D transition occurs for gold cluster anions. Although initially there was some controversy about the critical size for the 2D-3D transition,^{7,9} two recent work showed unequivocally the coexistence of 2D and 3D isomers in the beam of Au_{12}^- , based on combined trapped ion electron diffraction/DFT calculations³⁰ and PES using Ar-tagged Au_{12}^- .³¹ Figure 4(d) shows the 3D and 2D structures of Au_{12}^- (of C_{2v} and D_{3h} symmetry, respectively) and their simulated spectra with the inclusion of SO effect. Note that for open shell species such as Au_{12}^- , photodetachment from a fully occupied molecular orbital would result in both a triplet and a singlet final state. Such singlet-

triplet splitting cannot be reproduced well in the simulated spectra. Thus, the agreement between the experimental and simulated spectra for open-shell cluster anions is usually not as good as for those of closed-shell cluster anions. In the case of Au_{12}^- , the overall spectral patterns of the simulated spectra for both isomers [Fig. 4(d)] are in reasonably good agreement with the experimental data. It should be pointed out that although the experimental data suggest that the 3D structure (C_{2v}) should be the global minimum for Au_{12}^- , evidenced by its higher relative intensity, our DFT/PBE0 calculations show that the 3D structure is 0.414 eV above the 2D (D_{3h}) isomer. This result is consistent with the conclusion of Ref. 30 that DFT/PBE calculations are biased toward 2D structures. Again, we rechecked the relative energies of the C_{2v} and the D_{3h} isomers using the M06-L functional, which shows that the 3D structure (C_{2v}) is more stable than the 2D (D_{3h}) by 0.276 eV in agreement with the experimental observations.

For AgAu_{11}^- and CuAu_{11}^- , the experimental data [Figs. 4(b) and 4(c)] suggest unequivocally that only the 3D isomers derived from the C_{2v} global minimum of Au_{12}^- are observed. For CuAu_{11}^- , our calculations show that the C_{2v} - Au_{12}^- derived 3D structure is the global minimum, in which the Cu atom substitutes a hexacoordinated Au atom [inset in Fig. 4(f)]. The simulated spectrum of this isomer is nearly identical to that of the parent Au_{12}^- and is in good overall agreement with the observed PES spectrum. However, for AgAu_{11}^- , our calculations suggest that the first three low-lying structures are derived from the D_{3h} planar Au_{12}^- . The 3D AgAu_{11}^- structure [Fig. 4(e)] is structure IV, which is 0.176 eV higher in energy. These results are clearly inconsistent with the experimental observation, again due to the bias of the DFT/PBE0 calculation toward planar structures as revealed in the case of the parent Au_{12}^- .

The fact that the 2D isomers are not observed experimentally for the MAu_{11}^- clusters indicates that they are not competitive energetically. This observation is consistent with the conclusion that the Ag/Cu substitution has shifted the 2D-3D structural transition to a smaller cluster size, i.e., to the 11-atom clusters, MAu_{10}^- .

VI. CONCLUSIONS

In conclusion, we have presented a joint PES and DFT study of a series of isoelectronically doped gold clusters, MAu_n^- ($n=8-11$, $M=\text{Ag,Cu}$), which encompass the size range where the 2D-3D structural transition occurs for bare gold cluster anions. The combined experimental and computational results allow us to gain insight into the structural characteristics of the bimetallic species and the effects of doping on the structural evolution. The PES spectra of MAu_{10}^- and MAu_{11}^- are similar to those of the parent Au_{10}^- and Au_{11}^- clusters, respectively, suggesting that the dopant atom (Ag or Cu) simply substitutes one Au atom in the parent planar clusters without significant structural alterations. In both cases,

our DFT calculations show that the Cu atom prefers the central and hexa-coordinated sites, whereas the Ag atom prefers the low coordination edge sites. For Au_{10}^- we observe totally *four coexisting* low-lying planar isomers. The coexistence of so many low-lying isomers for the small-sized gold cluster Au_{10}^- is quite unprecedented. Interestingly, all the low-lying isomers of Au_{10}^- can be viewed as a central D_{6h} Au_7^- unit with the additional three Au atoms arranged in different positions around it. For MAu_{10}^- , the observed PES spectra are different from that of the parent Au_{11}^- cluster, suggesting a major structural transition. While the pure gold cluster Au_{11}^- is planar, we found that the doped clusters MAu_{10}^- are 3D, indicating an earlier 2D-3D transition in the doped clusters. For MAu_{11}^- , we only observed the 3D isomers, in contrast to the parent Au_{12}^- cluster for which both the 2D and 3D isomers coexist. Our results show that the isoelectronic substitution induces an earlier onset of 3D structures in gold clusters.

ACKNOWLEDGMENTS

The experimental work was supported by the National Science Foundation (Grant No. CHE-0749496). The theoretical work done at Washington using NWChem was performed on supercomputers at the EMSL Molecular Science Computing Facility. The theoretical work done at UNL was supported by grants from the National Science Foundation (Grant No. DMR-0820521), the Nebraska Research Initiative, and the University of Nebraska Holland Computing Center.

- ¹M. Haruta, *Catal. Today* **36**, 153 (1997).
- ²J. Ho, K. M. Ervin, and W. C. Lineberger, *J. Chem. Phys.* **93**, 6987 (1990).
- ³G. A. Bishea and M. D. Morse, *J. Chem. Phys.* **95**, 8779 (1991).
- ⁴G. F. Gantefor, D. M. Cox, and A. Kaldor, *J. Chem. Phys.* **96**, 4102 (1992).
- ⁵K. J. Taylor, C. L. Pettiettehall, O. Cheshnovsky, and R. E. Smalley, *J. Chem. Phys.* **96**, 3319 (1992).
- ⁶B. A. Collings, K. Athanassenas, D. Lacombe, D. M. Rayner, and P. A. Hackett, *J. Chem. Phys.* **101**, 3506 (1994).
- ⁷F. Furche, R. Ahlrichs, P. Weis, C. Jacob, S. Gilb, T. Bierweiler, and M. M. Kappes, *J. Chem. Phys.* **117**, 6982 (2002).
- ⁸S. Gilb, P. Weis, F. Furche, R. Ahlrichs, and M. M. Kappes, *J. Chem. Phys.* **116**, 4094 (2002).
- ⁹H. Häkkinen, B. Yoon, U. Landman, X. Li, H. J. Zhai, and L. S. Wang, *J. Phys. Chem. A* **107**, 6168 (2003).
- ¹⁰J. Li, X. Li, H. J. Zhai, and L. S. Wang, *Science* **299**, 864 (2003).
- ¹¹H. Häkkinen, M. Moseler, O. Kostko, N. Morgner, M. A. Hoffmann, and B. von Issendorff, *Phys. Rev. Lett.* **93**, 093401 (2004).
- ¹²M. Ji, X. Gu, X. Li, X. G. Gong, J. Li, and L. S. Wang, *Angew. Chem. Int. Ed.* **44**, 7119 (2005).
- ¹³S. Bulusu, X. Li, L. S. Wang, and X. C. Zeng, *Proc. Natl. Acad. Sci. U.S.A.* **103**, 8326 (2006); W. Huang, S. Bulusu, R. Pal, X. C. Zeng, and L. S. Wang, *ACS Nano* **3**, 1225 (2009).
- ¹⁴X. Xing, B. Yoon, U. Landman, and J. H. Parks, *Phys. Rev. B* **74**, 165423 (2006).
- ¹⁵X. Gu, S. Bulusu, X. Li, X. C. Zeng, J. Li, X. G. Gong, and L. S. Wang, *J. Phys. Chem. C* **111**, 8228 (2007).
- ¹⁶A. Lechtken, D. Schooss, J. R. Stairs, M. N. Blom, F. Furche, N. Morgner, O. Kostko, B. von Issendorff, and M. M. Kappes, *Angew. Chem., Int. Ed.* **46**, 2944 (2007).
- ¹⁷P. Gruene, D. M. Rayner, B. Redlich, A. F. G. van der Meer, J. T. Lyon, G. Meijer, and A. Fielicke, *Science* **321**, 674 (2008).
- ¹⁸P. Pyykkö, *Chem. Rev.* **88**, 563 (1988); *Inorg. Chim. Acta* **358**, 4113 (2005).
- ¹⁹I. L. Garzón, K. Michaelian, M. R. Beltrán, A. Posada-Amarillas, P. Ordejón, E. Artacho, D. Sánchez-Portal, and J. M. Soler, *Phys. Rev. Lett.*

- 81**, 1600 (1998).
- ²⁰ H. Häkkinen and U. Landman, *Phys. Rev. B* **62**, R2287 (2000).
- ²¹ R. Wesendrup, T. Hunt, and P. Schwerdtfeger, *J. Chem. Phys.* **112**, 9356 (2000).
- ²² H. Häkkinen, M. Moseler, and U. Landman, *Phys. Rev. Lett.* **89**, 033401 (2002).
- ²³ J. Wang, G. Wang, and J. Zhao, *Phys. Rev. B* **66**, 035418 (2002).
- ²⁴ M. P. Johansson, D. Sundholm, and J. Vaara, *Angew. Chem., Int. Ed.* **43**, 2678 (2004).
- ²⁵ R. M. Olson, S. Varganov, M. S. Gordon, H. Metiu, S. Chretien, P. Piecuch, K. Kowalski, S. A. Kucharski, and M. Musial, *J. Am. Chem. Soc.* **127**, 1049 (2005).
- ²⁶ A. V. Walker, *J. Chem. Phys.* **122**, 094310 (2005); L. Xiao and L. Wang, *Chem. Phys. Lett.* **392**, 452 (2004).
- ²⁷ S. Bulusu and X. C. Zeng, *J. Chem. Phys.* **125**, 154303 (2006).
- ²⁸ P. Koskinen, H. Häkkinen, B. Huber, B. von Issendorff, and M. Moseler, *Phys. Rev. Lett.* **98**, 015701 (2007); L. Xiao, B. Tollberg, X. Hu, and L. Wang, *J. Chem. Phys.* **124**, 114309 (2006).
- ²⁹ R. M. Olson and M. S. Gordon, *J. Chem. Phys.* **126**, 214310 (2007).
- ³⁰ M. P. Johansson, A. Lechtken, D. Schooss, M. M. Kappes, and F. Furche, *Phys. Rev. A* **77**, 053202 (2008).
- ³¹ W. Huang and L. S. Wang, *Phys. Rev. Lett.* **102**, 153401 (2009).
- ³² V. Bonačić-Koutecky, J. Burda, R. Mitrić, M. F. Ge, G. Zampella, and P. Fantucci, *J. Chem. Phys.* **117**, 3120 (2002).
- ³³ P. Weis, T. Bierweiler, S. Gilb, and M. M. Kappes, *Chem. Phys. Lett.* **355**, 355 (2002).
- ³⁴ E. M. Fernández, J. M. Soler, I. L. Garzon, and L. C. Balbas, *Phys. Rev. B* **70**, 165403 (2004).
- ³⁵ G. A. Bishea, C. A. Arrington, J. M. Behm, and M. D. Morse, *J. Chem. Phys.* **95**, 8765 (1991).
- ³⁶ P. Weis, O. Welz, E. Vollmer, and M. M. Kappes, *J. Chem. Phys.* **120**, 677 (2004).
- ³⁷ W. Bouwen, F. Vanhoutte, F. Despa, S. Bouckaert, S. Neukermans, L. T. Kuhn, H. Weidele, P. Lievens, and R. E. Silverans, *Chem. Phys. Lett.* **314**, 227 (1999).
- ³⁸ Y. Negishi, Y. Nakamura, A. Nakajima, and K. Kaya, *J. Chem. Phys.* **115**, 3657 (2001).
- ³⁹ K. Koyasu, Y. Naono, M. Akutsu, M. Mitsui, and A. Nakajima, *Chem. Phys. Lett.* **422**, 62 (2006).
- ⁴⁰ L. M. Wang, S. Bulusu, H. J. Zhai, X. C. Zeng, and L. S. Wang, *Angew. Chem., Int. Ed.* **46**, 2915 (2007).
- ⁴¹ L. M. Wang, R. Pal, W. Huang, X. C. Zeng, and L. S. Wang, *J. Chem. Phys.* **130**, 051101 (2009).
- ⁴² W. Huang, R. Pal, L. M. Wang, X. C. Zeng, and L. S. Wang, *J. Chem. Phys.* **132**, 054305 (2010).
- ⁴³ C. W. Bauschlicher, S. R. Langhoff, and H. Partridge, *J. Chem. Phys.* **91**, 2412 (1989).
- ⁴⁴ V. Kellö and A. J. Sadlej, *J. Chem. Phys.* **103**, 2991 (1995).
- ⁴⁵ S. Zorriasatein, K. Joshi, and D. G. Kanhere, *J. Chem. Phys.* **128**, 184314 (2008).
- ⁴⁶ H. M. Lee, M. F. Ge, B. R. Sahu, P. Tarakeshwar, and K. S. Kim, *J. Phys. Chem. B* **107**, 9994 (2003).
- ⁴⁷ G. F. Zhao and Z. Zeng, *J. Chem. Phys.* **125**, 014303 (2006).
- ⁴⁸ M. J. López, P. A. Marcos, and J. A. Alonso, *J. Chem. Phys.* **104**, 1056 (1996).
- ⁴⁹ S. Darby, T. V. Mortimer-Jones, R. L. Johnston, and C. Roberts, *J. Chem. Phys.* **116**, 1536 (2002); A. Rapallo, G. Rossi, R. Ferrando, A. Fortunelli, B. C. Curley, L. D. Lloyd, G. M. Tarbuck, and R. L. Johnston, *ibid.* **122**, 194308 (2005).
- ⁵⁰ Y. Gao, N. Shao, Y. Pei, and X. C. Zeng, *Nano Lett.* **10**, 1055 (2010).
- ⁵¹ L. S. Wang, H. S. Cheng, and J. W. Fan, *J. Chem. Phys.* **102**, 9480 (1995).
- ⁵² D. J. Wales and H. A. Scheraga, *Science* **285**, 1368 (1999).
- ⁵³ B. J. Delley, *Chem. Phys.* **92**, 508 (1990).
- ⁵⁴ J. P. Perdew, K. Burke, and M. Ernzerhof, *Phys. Rev. Lett.* **77**, 3865 (1996).
- ⁵⁵ S. Yoo and X. C. Zeng, *J. Chem. Phys.* **119**, 1442 (2003); *Angew. Chem., Int. Ed.* **44**, 1491 (2005).
- ⁵⁶ R. B. Ross, J. M. Powers, T. Atashroo, W. C. Ermler, L. A. LaJohn, and P. A. Christiansen, *J. Chem. Phys.* **93**, 6654 (1990).
- ⁵⁷ W. Huang, S. Bulusu, R. Pal, X. C. Zeng, and L. S. Wang, *J. Chem. Phys.* **131**, 234305 (2009).
- ⁵⁸ R. A. Kendall, E. Aprà, D. E. Bernholdt, E. J. Bylaska, M. Dupuis, G. I. Fann, R. J. Harrison, J. Ju, J. A. Nichols, J. Nieplocha, T. P. Straatsma, T. L. Windus, and A. T. Wong, *Comput. Phys. Commun.* **128**, 260 (2000).
- ⁵⁹ E. J. Bylaska, W. A. de Jong, N. Govind, K. Kowalski, T. P. Straatsma, M. Valiev, D. Wang, E. Apra, T. L. Windus, J. Hammond, P. Nichols, S. Hirata, M. T. Hackler, Y. Zhao, P.-D. Fan, R. J. Harrison, M. Dupuis, D. M. A. Smith, J. Nieplocha, V. Tipparaju, M. Krishnan, Q. Wu, T. Van Voorhis, A. A. Auer, M. Nooijen, E. Brown, G. Cisneros, G. I. Fann, H. Fruchtl, J. Garza, K. Hirao, R. Kendall, J. A. Nichols, K. Tsemekhman, K. Wolinski, J. Anchell, D. Bernholdt, P. Borowski, T. Clark, D. Clerc, H. Dachsel, M. Deegan, K. Dyall, D. Elwood, E. Glendening, M. Gutowski, A. Hess, J. Jaffe, B. Johnson, J. Ju, R. Kobayashi, R. Kutteh, Z. Lin, R. Littlefield, X. Long, B. Meng, T. Nakajima, S. Niu, L. Pollack, M. Rosing, G. Sandrone, M. Stave, H. Taylor, G. Thomas, J. van Lenthe, A. Wong, and Z. Zhang, *NWChem, A Computational Chemistry Package for Parallel Computers, Version 5.1* (Pacific Northwest National Laboratory, Richland, 2009).
- ⁶⁰ W. Huang and L. S. Wang, *Phys. Chem. Chem. Phys.* **11**, 2663 (2009).
- ⁶¹ H. Häkkinen, *Chem. Soc. Rev.* **37**, 1847 (2008).
- ⁶² E. Janssens, H. Tanaka, S. Neukermans, R. E. Silverans, and P. Lievens, *New J. Phys.* **5**, 46 (2003).
- ⁶³ See supplementary material at [10.1063/1.3356046](https://doi.org/10.1063/1.3356046) for more information on structures, relative energies, and simulated photoelectron spectra of low-lying isomers of AgAu_{10}^- and CuAu_{10}^- .
- ⁶⁴ L. Ferrighi, B. Hammer, and G. K. H. Madsen, *J. Am. Chem. Soc.* **131**, 10605 (2009).
- ⁶⁵ M. Mantina, R. Valero, and D. G. Truhlar, *J. Chem. Phys.* **131**, 064706 (2009).